Organic & Biomolecular Chemistry

PAPER

View Article Online
View Journal

Cite this: DOI: 10.1039/c5ob00676g

Synthesis and properties of unsymmetrical azatrioxa[8]circulenes†

Malene Plesner, Thomas Hensel, Bjarne E. Nielsen, Fadhil S. Kamounah, Theis Brock-Nannestad, Christian B. Nielsen, Christian G. Tortzen, Ole Hammerich and Michael Pittelkow*

Received 6th April 2015,
Accepted 21st April 2015

DOI: 10.1039/c5ob00676g

www.rsc.org/obc

Insights to the subtle reactivity patterns of hydroxy-substituted carbazoles allows the precise synthesis of unsymmetrical azatrioxa[8]circulenes by the reaction of *N*-benzyl-2,7-di-*tert*-butyl-3,6-dihydroxycarbazole with two different 1,4-benzoquinones in the presence of an oxidant (chloranil) and a Lewis acid (BF_3OEt_2). The unique synthetic control obtained originates from the selectivity obtained upon reacting *N*-benzyl-2,7-di-*tert*-butyl-3,6-dihydroxycarbazole with an electron-rich benzoquinone to give first the C–C bond formation and then subsequently the dibenzofuran formation with high regioselectivity. Herein the first synthesis of unsymmetrical antiaromatic azatrioxa[8]circulenes and the full characterization using NMR spectroscopy, optical spectroscopy, electrochemistry, computational techniques and single crystal X-ray crystallography is reported. The controlled stepwise condensation of *N*-benzyl-2,7-di-*tert*-butyl-3,6-dihydroxycarbazole with two different 1,4-benzoquinones gives selectively the unsymmetrical azatrioxa[8]circulenes.

Introduction

Classical aromatic compounds such as benzene obey Hückel's $4n + 2$ π-electron rule, while anti-aromatic compounds have $4n$ π-electrons.[1,2] The idea of extending the π-conjugated framework of polycyclic aromatic- and heteroaromatic molecules has fascinated chemists for more than a century.[3] An interest in the exploration of fundamental properties inspired early studies of structure–property relationships, while more recent work has focused on using π-conjugated compounds as the active materials in optical and electronic devices.[3] Recent work by Haley[4] on the preparation of indeno[1,2-*b*]fluorenes, by Osuka,[5] Sessler[6] and Latos-Grażyński[7] on the preparation of porphyrioids, and by Bunz[9] on the preparation of heteroacenes have paved the way to studies of the properties of large polycyclic aromatic-antiaromatic conjugates.[19]

Planarized conjugated cyclooctatetraenes (COTs) are among the classic antiaromatic moieties, and as part of heterocyclic [8]circulenes COTs have attracted the interest of Komatsu,[8] Osuka,[10] Nenajdenko,[11] Wong,[12] Christensen,[13] Erdtman and Högberg,[14] and us.[15] We have previously used DTF based nuclear independent chemical shift (NICS) calculations on the diazadioxa[8]circulenes (**1**), azatrioxa[8]circulenes (**2**) and tetraoxa[8]circulenes (**3**) to address the question of the aromaticity/antiaromaticity of the central planarized COTs, and found that the COT indeed possess anti-aromatic character.[16] Another feature that we have explored with heterocyclic [8]circulenes is their (blue) fluorescent properties. We have found that the azatrioxa[8]circulenes and the diazadioxa[8]circulenes fluoresce in the blue region making them attractive for application in light emitting devices.[17] Aggregation of π-conjugated systems tends to shift the fluorescence from the blue to the green region, and we have found it useful to functionalize the [8]circulenes with *tert*-butyl groups to modulate aggregation behaviour.[18]

The previously described synthetic methodologies developed for heterocyclic [8]circulenes limit the range of compounds available to symmetrical structures. Preparing unsymmetrical π-extended heterocyclic[8]circulenes may open the possibility of systematically studying the interplay between aromatic and antiaromatic moieties in large π-conjugated frameworks. In this paper we showcase a new synthetic protocol towards this goal, and we report on the spectroscopic, computational and electrochemical properties. The work described in this paper focuses on utilizing the intrinsic reactivity of hydroxyl-substituted carbazoles for the construction of azatrioxa[8]circulenes. We have found that we can modulate the reactivity of the hydroxyl-substituted carbazoles by careful choice of benzoquinone reaction partners, and thus opening the pathway for construction of complex heterocyclic [8]circulenes.

Department of Chemistry, University of Copenhagen, Universitetsparken 5, DK-2100 Copenhagen Ø, Denmark. E-mail: pittel@kiku.dk

†Electronic supplementary information (ESI) available: NMR spectra for new compounds, general experimental procedures, a detailed NMR assignment and further electrochemical assignments. CCDC 1032471. For ESI and crystallographic data in CIF or other electronic format see DOI: 10.1039/c5ob00676g

Results and discussion

The synthetic strategy is built upon the observation that 1,4-benzoquinones tetramerize by treatment with acid to yield tetraoxa[8]circulenes **3** *via* a 3,6-dihydroxydibenzofuran intermediate.[17] Recently we applied a similar logic and condensed a 3,6-dihydroxycarbazole with two equivalents of suitable substituted 1,4-benzoquinones in the presence of a Lewis acid to give azatrioxa[8]circulenes (**2**, Scheme 1, middle) in high yields.[15a]

We found that the 3,6-dihydroxycarbazole may be dimerized under oxidative conditions to yield diazadioxa[8]circulenes **1** by simply changing from a 1,4-benzoquinone substituted with electron donating substituents to 1,4-benzoquinones substituted with electron withdrawing substituents (**1**, Scheme 1, top).[15b] It is important that the 1,4-benzoquinones are substituted in the 2- and 3-positions and that the 3,6-dihydroxycarbazole is substituted in the 2- and 7-positions, as otherwise the reaction gives uncontrolled polymerisation.

When *N*-benzyl-2,7-di-*tert*-butyl-3,6-dihydroxycarbazole (**4**) is treated with only one equivalent of a 1,4-quinone that does not cause it to dimerize (the benzoquinone should not have an electron-withdrawing substituent) to the diazadioxa[8]circulene (**1**) the reaction mixture contains mainly the product where one C–C bond has been formed (**5**, Scheme 2, top).

Addition of one equivalent of an oxidant such as chloranil to the tetrahydroxy compound **5** in the presence of BF_3OEt_2 yields the ring-closed furan **6**. Subsequent addition of a second 1,4-quinone to this material gives the unsymmetrical azatrioxa[8]circulene **2** in a process where two new C–C bonds and two furan rings are formed (Scheme 2, bottom).

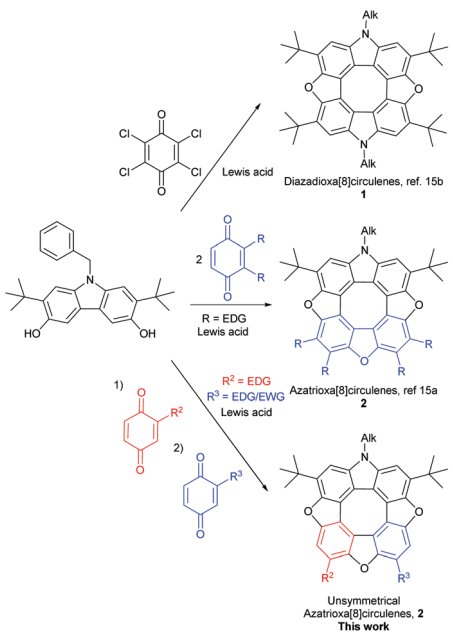

Scheme 1 Logic of diazadioxa[8]circulene (**1**)[15b] and azatrioxa[8]circulene (**2**)[15a] synthesis.

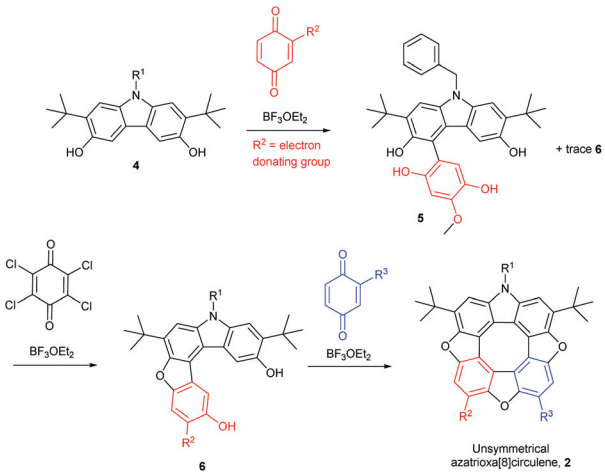

Scheme 2 Pathway to unsymmetrical azatrioxa[8]circulene. R^2 of the first 1,4-benzoquinone must be an electron donating group, otherwise the diazadioxa[8]circulene (**1**) is the main product.

We have found that when using either 2-*tert*-butyl-1,4-benzoquinone or 2-methoxy-1,4-benzoquinone only one regioisomer of the tetrahydroxy compound **5** was formed, and as a consequence only one regioisomer of the dibenzofuran **6** is formed after oxidation. Thus, the R^2 group is situated in the position indicated in Scheme 2 (red). When treating the *tert*-butyl derivative **5** generated *in situ* with either 2-methoxy-1,4-benzoquinone (43%), 2-thiododecyl-1,4-benzoquinone (35%, 2-*tert*-butyl-1,4-benzoquinone (13%) or 1,4-naphthoquinone (31%) we isolate the unsymmetrical azatrioxa[8]circulenes (**2**, Fig. 1) in good yields.

In all three cases where unsymmetrical azatrioxa[8]circulenes are made, one regioisomer is formed as the main product. This is a remarkable control of regiochemistry in a

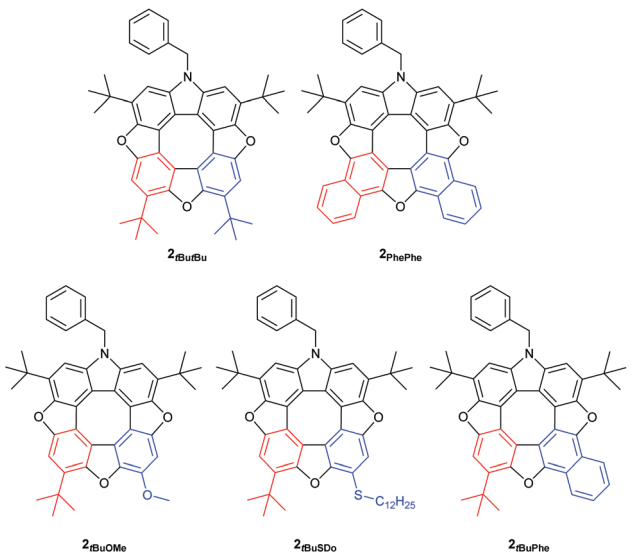

Fig. 1 Azatrioxa[8]circulenes (**2**) described in this paper.

reaction protocol where three C–C bonds and three C–O bonds are formed while three molecules of water are eliminated. When starting by reacting the *N*-benzyl-2,7-di-*tert*-butyl-3,6-dihydroxycarbazole (**4**) with 2-methoxy-1,4-benzoquinone followed by 2-*tert*-butyl-1,4-benzoquinone it gave exactly the same azatrioxa[8]circulene product as when the reaction was performed with the reverse order, as seen by ^{1}H-NMR analysis of the isolated pure product. We have also found that if the sequence is started by reacting the *N*-benzyl-2,7-di-*tert*-butyl-3,6-dihydroxycarbazole (**4**) with 1,4-naphthoquinone, and then with 2-*tert*-butyl-1,4-benzoquinone, then we obtained a mixture of the two azatrioxa[8]circulene regioisomers with respect to the *tert*-butyl group originating from the 2-*tert*-butyl-1,4-benzoquinone.

The unsymmetrical azatrioxa[8]circulenes were all crystalline compounds, however we were not able to grow crystals with large enough dimensions to be suitable for single crystal X-ray crystallography. We were able to grow crystals of the C_2-symmetrical azatrioxa[8]circulene ($\mathbf{2}_{t\mathbf{Bu}t\mathbf{Bu}}$, Fig. 2). The single crystal X-ray structure confirms outcome of the azatrioxa[8]-circulenes synthesis and also the regiochemical outcome of the reaction forming the azatrioxa[8]circulene with respect to the *tert*-butyl groups originating from the 2-*tert*-butyl-benzoquinones. The azatrioxa[8]circulene is planar with respect to the π-conjugated system and due to the four *tert*-butyl substituents no intermolecular π–π-stacking is observed.

We have previously performed NICS calculations on planar heterocyclic [8]circulenes (**1**–**3**) in order to address the question of the antiaromaticity of the central planarized COTs.[15,16] NICS(0) and NICS(1)$_{zz}$ values for $\mathbf{2}_{t\mathbf{BuOMe}}$ were determined at the B3LYP/6-311+G(d,p) level of theory using geometries obtained from B3LYP/6-31G(d) confirming the antiaromatic nature of the COT (Fig. 3).

The UV/Vis and fluorescence spectra of the series of new azatrioxa[8]circulene **2** were recorded to assess whether these derivatives would be suitable for applications as the fluorescent component in blue OLEDs (Fig. 4). Three common electronic transitions are centered at ~260 nm (~4.8 eV), ~360 nm (~3.4 eV) and at ~425 nm (~2.9 eV) with varying intensities.

The oscillator strength and Franck–Condon factors for each transition are not identical when comparing the transitions at

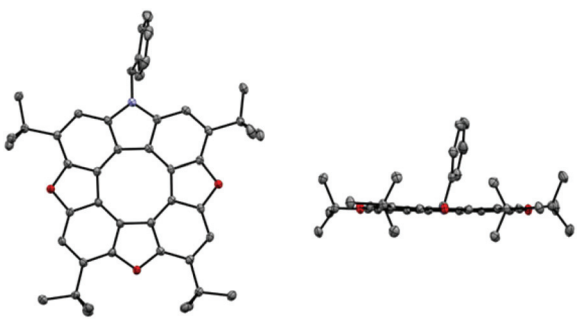

Fig. 2 Single crystal X-ray structure of azatrioxa[8]circulene ($\mathbf{2}_{t\mathbf{Bu}t\mathbf{Bu}}$). Hydrogens are omitted for clarity. Left: top view. Right: side view.

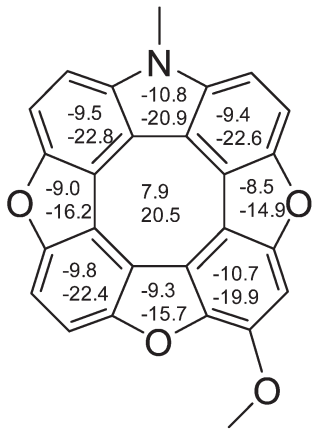

Fig. 3 NICS(0) and NICS(1)$_{zz}$ (lower numbers) values calculated for the methoxy substituted azatrioxa[8]circulene (**2**).

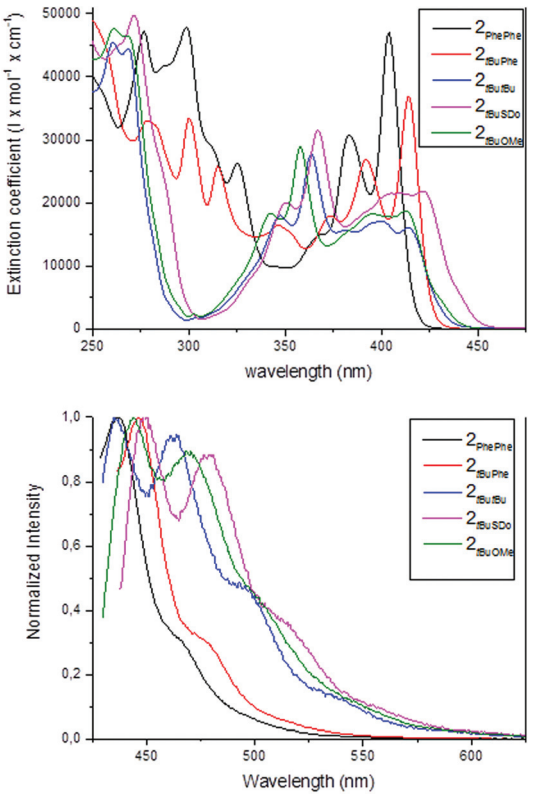

Fig. 4 UV/Vis (top) and normalized fluorescence spectra (bottom) of the series of azatrioxa[8]circulenes (CH_2Cl_2).

the low energy transition. The transition at ~425 nm is weak in intensity in the spectrum of the three azatrioxa[8]circulenes without a naphthalene units (extinction coefficient of 15 000–20 000 M^{-1} cm^{-1}) compared to the spectra of the two azatrioxa[8]circulenes with either one or two naphthalene moieties (extinction coefficients of ~35 000–45 000 M^{-1} cm^{-1}). The two C_2 symmetrical azatrioxa[8]circulenes ($\mathbf{2}_{\mathbf{PhePhe}}$ and $\mathbf{2}_{t\mathbf{ButBu}}$) have a slightly blue-shifted fluorescence as compared to the

three unsymmetrical azatrioxa[8]circulenes. Again the two azatrioxa[8]circulenes containing naphthalene units ($\mathbf{2_{PhePhe}}$ and $\mathbf{2_{tBuPhe}}$) give fluorescence spectra with comparable features, but the spectrum of the compound containing two naphthalenes is blue-shifted by *ca.* 20 nm. The fluorescence spectra of the three unsymmetrical azatrioxa[8]circulenes with identical π-systems ($\mathbf{2_{tBuOMe}}$, $\mathbf{2_{tBuSDo}}$ and $\mathbf{2_{tBu}}$$\mathbf{_{tBu}}$) have similar features, with the high-energy bands of the $\mathbf{2_{tBuOMe}}$ (10 nm) and $\mathbf{2_{tBuSDo}}$ (15 nm) slightly redshifted as compared to $\mathbf{2_{tBu}}$$\mathbf{_{tBu}}$. We also determined the fluorescence quantum yields for the series, and the quantum yields increase significantly with the increasing area of the π-conjugated system (Table 1).

The optical data suggests that the π-extended azatrioxa[8]-circulenes may be suitable candidates as the fluorescent component in light emitting devices, as this derivative fluoresce in the blue region and it does not aggregate in solution. Analysis of the crystal structure of $\mathbf{2_{PhePhe}}$ [15a] suggests that this derivative aggregates in the solid state, so despite having the highest quantum yield of fluorescence it may be more desirable to utilize the $\mathbf{2_{tBuPhe}}$ derivative in light emitting devices.

The electrochemical oxidation of the five compounds was studied by cyclic voltammetry in dichloromethane with $(n\mathrm{Bu})_4\mathrm{PF}_6$ (0.1 M) as the supporting electrolyte. Reversible one-electron oxidations corresponding to the formation of persistent radical cations were observed for $\mathbf{2_{tBuOMe}}$, $\mathbf{2_{tBuSDo}}$, $\mathbf{2_{tBuPhe}}$ and $\mathbf{2_{tBu}}$$\mathbf{_{tBu}}$ (Fig. S14†). In the case of $\mathbf{2_{PhePhe}}$, the oxidation process appeared as a double peak composed of two closely spaced electron transfer processes (Fig. 5). The voltammogram gradually developed into that for a simple one-electron transfer upon dilution. In contrast, the double peak behaviour became increasingly pronounced with decreasing temperature (Fig. S15†). Similar observations were recently reported for indenofluorene-extended tetrathiafulvalenes and were shown to originate from the formation of radical cation-neutral and radical cation-radical cation associates.[20] It is likely that similar associates result from the oxidation of $\mathbf{2_{PhePhe}}$ that in contrast to the four other members of the series has one dibenzofuran subunit not carrying a space filling *tert*-butyl group, but rather an extended π-system resulting from the presence of two additional benzene rings. The values of the formal potentials for the one-electron oxidations are summarized in Table 1 and it is seen that the minor structural changes that distinguish the five azatrioxa[8]circulenes are reflected by oxidation potentials that are very similar. A second oxidation wave corresponding to the subsequent formation of the dication was observed close to the solvent wall for all compounds (Fig. S16†). For $\mathbf{2_{tBuSDo}}$ the dication was observed to react with residual water; deprotonation resulted in the formation of the corresponding *S*-oxide that was further oxidized to a persistent radical cation at the potential of the second wave (Fig. S17†).

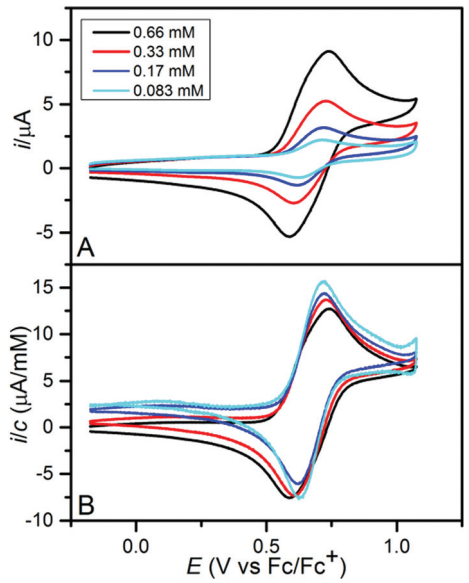

Fig. 5 The influence of the substrate concentration (see the insert) on the shape of the cyclic voltammogram for $\mathbf{2_{PhePhe}}$. (A) the raw data and (B) the same data after background subtraction and normalization with respect to the substrate concentration. The working electrode was a circular glassy carbon disk (d = 3 mm); the voltage sweep rate was 0.1 V s^{-1}.

Table 1 Quantum yields and electrochemical data

Compound	Quantum yield[a]	Oxidation potential[b]
$\mathbf{2_{PhePhe}}$	0.89	0.67 V
$\mathbf{2_{tBu}}$$\mathbf{_{tBu}}$	0.31	0.67 V
$\mathbf{2_{tBuOMe}}$	0.17	0.62 V
$\mathbf{2_{tBuSDo}}$	0.28	0.66 V
$\mathbf{2_{tBuPhe}}$	0.67	0.65 V

[a] Quantum yields determined in CH_2Cl_2. [b] Formal potentials determined by cyclic voltammetry as the average of E_p^{ox} and E_p^{red} for the first oxidation wave. Solvent: dichloromethane, supporting electrolyte: $(n\mathrm{Bu})_4\mathrm{PF}_6$ (0.1 M), voltage sweep rate: 0.1 V s^{-1}, working electrode: glassy carbon (d = 3 mm).

Conclusion

In summary, we have developed a novel synthetic method for the preparation of a series of unsymmetrical azatrioxa[8]circulenes and have demonstrated the feasibility of functionalising fully conjugated, formally antiaromatic azatrioxa[8]circulenes. Through X-ray crystallography and DFT calculations we have visualised the planar COT core and confirmed the structure of **2** by comparison to the other known molecules that contain this moiety. Examination of the optoelectronic properties of the series of azatrioxa[8]circulenes unambiguously confirms that the optical properties of this antiaromatic framework can modulated by careful design.

Experimental section

All chemicals and solvents, unless otherwise stated, were purchased from commercial suppliers and used as received. Analytical thin layer chromatography (TLC) was performed on

SiO_2 plates and visualized under UV-light (254 or 360 nm). Dry column vacuum chromatography was carried out using SiO_2 (60 Å, 15–40 μm). NMR spectra were recorded on a 500 MHz spectrometer. Temperature dependent NMR spectra were recorded on a 300 MHz spectrometer. 1H NMR and 13C NMR spectra were recorded at 500 MHz and 125 MHz, respectively, on a 500 spectrometer using residual non-deuterated solvent as the internal standard. All chemical shifts (δ) are quoted in ppm and all coupling constants (J) are expressed in Hertz (Hz). The following abbreviations are used for convenience in reporting the multiplicity for NMR resonances: s = singlet, bs = broad singlet, d = doublet, t = triplet, q = quartet, and m = multiplet. Samples were prepared using $CDCl_3$ or DMSO-d6. Assignment of all ^1H and ^{13}C resonances was achieved using standard 2D NMR techniques as ^1H–^1H COSY, ^1H–^{13}C HSQC, and ^1H–^{13}C HMBC. Elemental analysis was conducted at the Department of Chemistry, University of Copenhagen. MALDI-TOF MS was recorded using dithranol as matrix. The MALDI HRMS was recorded using dithranol as matrix, and calibration was performed externally, using sodium trifluoroacetate cluster ions. UV-Vis and fluorescence spectra were measured in CH_2Cl_2. Cyclic voltammetry was carried out at 5×10^{-4} mol L^{-1}. $(n\mathrm{Bu})_4NPF_6$ (1 M) was used as supporting electrolyte. The working electrode was a circular glassy carbon disk (d = 3 mm). A Pt-wire served as the counter electrode and the reference electrode was Ag/Ag^+. The potential scale was subsequently calibrated by recording the potential of the ferrocene/ferrocenium redox couple. The voltage sweep rate was 0.1 V s^{-1} and all experiments were carried out at room temperature unless otherwise stated. The geometry optimization was performed by the DFT B3LYP/6-31G(d) level using the GAUSSIAN 03 package. Based on the calculated coordinates of the ring critical points of the (3, +1) type the NICS (0) and NICS(1) indices are calculated by the B3LYP/6-311+G(d,p) level with the gauge-independent atomic orbital (GIAO) approach. Negative NICS values in the center of the ring corresponds to the presence of the "aromatic" diatropic ring currents, whereas positive NICS values at the same points denote the "antiaromatic" paratropic ring currents.

2-Methoxy-1,4-benzoquinone

In a 100 ml round bottomed flask was placed silica for flash column chromatography (6 g) and the flask was equipped with a magnet and sealed with a rubber septum. Cerium ammonium nitrate (2.75 g: 5.02 mmol) dissolved in water (3 ml) was added drop wise whilst the silica was stirred using magnetic stirring. The silica was stirred for an additional 5 min. CH_2Cl_2 (25 ml) was added followed by the addition of 2-methoxy-1,4-hydroquinone (280 mg: 2.00 mmol) suspended in CH_2Cl_2 (5 ml). The reaction mixture was stirred for 30 minutes and filtered through a sintered glass funnel. The filter cake was washed with CH_2Cl_2 (3 × 50 ml) and the solvent was removed from the combined filtrates yielding 2-methoxy-1,4-benzoquinone, fine yellow powder.

Yield: 96% (266 mg: 1.92 mmol) melting point: 47–49 °C TLC: R_f-value = 0.26 (CH_2Cl_2) ^{1}H-NMR (500 MHz, $CDCl_3$): δ = 6.71 (m, 2H), 5.95 (s, 1H), 3.83 (s, 3H) ppm. ^{13}C-NMR (126 MHz, $CDCl_3$): δ = 187.6 (C_q), 181.9 (C_q), 158.8 (C_q), 137.4 (*C*H), 134.6 (*C*H), 107.9 (*C*H), 56.4 (–O*C*H$_3$) ppm. Elemental analysis: C: 60.90%, H: 4.10%, N: 0% (theoretical – C: 60.87%, H: 4.38% N: 0%). GC-MS: calcd for $C_7H_6O_3$ $[M]^+$ m/z 138.0, found 138.1.

***N*-Benzyl-2,7-di-*tert*-butyl-9*H*-carbazole-3,6-diol (4).** *N*-Benzyl-2,7-di-*tert*-butyl-3,6-dimethoxy-9*H*-carbazole (1.002 g: 2.33 mmol) and tetra-*n*-butylammonium iodide (1.678 g: 4.54 mmol) were placed in a round bottomed flask under a nitrogen atmosphere. Boron trichloride (22 ml: 1 M in CH_2Cl_2, 22 mmol) was added over the course of 5 minutes and the reaction mixture was stirred using magnetic stirring for 1 h 15 min. The reaction was quenched using 1 M HCl (150 ml) and extracted with CH_2Cl_2 (6 × 70 ml). After drying the combined organic phase over Na_2SO_4 and filtration the solvent was removed under vacuum. The resulting yellow-brown foam was purified by dry column vacuum chromatography [id 4 cm; 4 cm silica; 100 cm^3 fractions; 0–12% MeCN in toluene (v/v) – 2% increments] yielding *N*-benzyl-2,7-di-*tert*-butyl-9*H*-carbazole-3,6-diol (**6**), fine white powder.

Yield: 82.5% (773 mg: 1.92 mmol) melting point: 205–209 °C TLC: R_f-value = 0.35 (MeCN/toluene, 1 : 8) ^{1}H-NMR (500 MHz, DMSO): δ = 8.87 (s, 2H, 2 × RO*H*), 7.28 (t, J = 7.4 Hz, 2H), 7.24 (s, 2H), 7.23 (s, 2H), 7.22–7.17 (m, 3H), 5.46 (s, 2H, R_2NCH_2Ph), 1.40 (s, 18H, 2 × RC(C*H*$_3$)$_3$) ppm. ^{13}C-NMR (126 MHz, DMSO): δ = 149.2 (C_q), 138.7 (C_q), 134.8 (C_q), 134.6 (CH), 128.5 (C_q), 127.1 (CH), 126.9 (CH), 119.7 (CH), 106.7 (CH), 105.6 (CH), 45.7 (CH_2), 35.0 (C_q), 29.7 (CH_3) ppm. Elemental analysis: C: 81.00%, H: 7.76%, N: 3.41% (theoretical – C: 80.76%, H: 7.78% N: 3.49%), MALDI HRMS: calcd for $C_{27}H_{31}NO_2$ $[M]^+$ m/z 401.23 548, found 401.23464.

***N*-Benzyl-di-*tert*-butyl-di-naphtho-azatrioxa[8]circulene, 2_{PhePhe}.** *N*-Benzyl-2,7-di-*tert*-butyl-9*H*-carbazole-3,6-diol (383 mg: 0.95 mmol) and naphtoquinone (149 mg: 0.95 mmol) were dissolved in CH_2Cl_2 (50 ml) and placed under a nitrogen atmosphere. BF_3OEt_2 (0.07 ml: 0.45 mmol) was added to the reaction mixture in one portion and the reaction mixture was stirred for 1 hour. Naphtoquinone (226 mg: 1.43 mmol) and BF_3OEt_2(0.07 ml: 0.45 mmol) was added and the reaction mixture was stirred overnight. The reaction was quenched using 1 M HCl (100 ml) and KOH pellets were added until the water phase was alkaline. Extraction with CH_2Cl_2 (5 × 70 ml) was performed and the combined organic phase was dried over anhydrous Na_2SO_4 and filtered. The solvent was removed under vacuum and the brown crude product was purified by dry column vacuum filtration [id 4 cm; 1.5 cm silica; 25% toluene in heptane(v/v)] yielding *N*-benzyl-di-*tert*-butyl-di-naphtho-azatrioxa[8]circulene (**7**) as a yellow powder.

Yield: 49% (309 mg: 0.48 mmol) melting point: 304–308 °C TLC: R_f-value = 0.57 (toluene/*n*-heptane, 1 : 4) ^{1}H-NMR (500 MHz, $CDCl_3$): δ = 8.71–8.63 (m, 4H), 7.77–7.70 (m, 4H), 7.49 (s, 2H), 7.36–7.29 (m, 5H), 5.81 (s, 2H), 1.78 (s, 18H) ppm. ^{13}C-NMR (126 MHz, $CDCl_3$): δ = 150.5 (C_q), 148.9 (C_q), 148.8 (C_q), 137.9 (C_q), 137.6 (C_q), 134.1 (C_q), 129.0 (*C*H), 127.7 (*C*H), 126.9 (*C*H), 126.2 (*C*H), 126.0 (*C*H), 122.2 (*C*H), 121.9 (*C*H),

121.0 (C_q), 120.8 (C_q), 117.4 (C_q), 114.1 (C_q), 113.1 (C_q), 112.6 (C_q), 104.9 (*C*H), 47.8 (*C*H_2), 35.5 (*C*$(CH_3)_3$), 30.7 (R-*C*H_3) ppm. MALDI HRMS: calcd for $C_{47}H_{35}NO_3$ $[M]^+$ *m*/*z* 661.26169, found 661.26095.

***N*-Benzyl-tetra-*tert*-butyl-azatrioxa[8]circulene, 2$_{tButBu}$.** *N*-Benzyl-2,7-di-*tert*-butyl-9*H*-carbazole-3,6-diol (200 mg: 0.50 mmol) and 2-*tert*-butyl-1,4-benzoquinone (82 mg: 0.50 mmol) were dissolved in CH_2Cl_2 (50 ml) and placed under a nitrogen atmosphere. BF_3OEt_2 (0.13 ml: 1.00 mmol) was added to the reaction mixture in one portion and the reaction mixture was stirred for 5 hours. 2-*tert*-Butyl-1,4-quinone (123 mg: 0.75 mmol) was added and the reaction mixture was stirred for overnight. The reaction was quenched using 1 M HCl (100 ml) and KOH pellets were added until the water phase was alkaline (pH-paper). Extraction with CH_2Cl_2 (4 × 50 ml) was performed and the combined organic phase was dried over anhydrous Na_2SO_4 and filtered. The solvent was removed under vacuum and the brown crude product was purified by dry column vacuum filtration [id 4 cm; 4 cm silica; 65 cm^3 fractions, toluene in heptane (v/v) 0–10%, 2% increments] yielding *N*-benzyl-tetra-*tert*-butyl-azatrioxa[8]circulene (**8**) as a fine yellow powder.

Yield: 13% (45 mg: 0.06 mmol) melting point: 245–248 °C TLC: R_f-value = 0.69 (toluene/*n*-heptane, 1 : 4) ^{1}H-NMR (500 MHz, $CDCl_3$): δ = 7.73 (s, 2H), 7.39 (s, 2H), 7.36–7.27 (m, 5H), 5.75 (s, 2H), 1.77 (s, 18H), 1.69 (s, 18H) ppm. ^{13}C-NMR (126 MHz, $CDCl_3$): δ = 152.9 (C_q), 151.3 (C_q), 151.1 (C_q), 138.0 (C_q), 137.3 (C_q), 134.8 (C_q), 134.3 (C_q), 129.0 (*C*H), 127.7 (*C*H), 126.9 (*C*H), 117.1 (C_q), 116.8 (C_q), 115.1 (C_q), 112.7 (C_q), 107.4 (*C*H), 105.5 (*C*H), 47.8 (*C*H_2), 35.4 (C_q), 35.3 (C_q), 30.5 (*C*H_3) 30.4 (*C*H_3) ppm. MALDI HRMS: calcd for $C_{47}H_{47}NO_3$ $[M]^+$ *m*/*z* 673.35559, found 673.35398.

***N*-Benzyl-tri-*tert*-butyl-naphto-azatrioxa[8]circulene, 2$_{tBuPhe}$.** *N*-Benzyl-2,7-di-*tert*-butyl-9*H*-carbazole-3,6-diol (111 mg: 0.28 mmol) and 2-*tert*-butyl-1,4-quinone (47 mg: 0.28 mmol) were dissolved in CH_2Cl_2 (50 ml) and placed under a nitrogen atmosphere. BF_3OEt_2 (0.02 ml: 0.16 mmol) was added to the reaction mixture and the reaction mixture was stirred for 4 hours. Naphtoquinone (67 mg: 0.41 mmol) and BF_3OEt_2 (0.02 ml: 0.16 mmol) was added and the reaction mixture was stirred overnight. The reaction was quenched using 0.5 M HCl (75 ml) and KOH pellets were added until the water phase was alkaline. Extraction with CH_2Cl_2 (4 × 50 ml) was performed and the combined organic phase was dried over anhydrous Na_2SO_4 and filtered. The solvent was removed under vacuum and the brown crude product was purified by dry column vacuum filtration [id 4 cm; 1.5 cm silica; 50 cm^3 fractions, 0–30% toluene in heptane(v/v), 5% increments] yielding *N*-benzyl-tri-*tert*-butyl-naphtho-azatrioxa[8]circulene (**9**), as a fine yellow powder.

Yield: 31% (60 mg: 0.09 mmol) melting point: 300–303 °C TLC: R_f -value = 0.66 (toluene/*n*-heptane, 1 : 4) ^{1}H-NMR (500 MHz, $CDCl_3$): δ = 8.71–8.66 (m, 2H, Ar*H*), 7.79 (s, 1H), 7.76 (dt, *J* = 6.3, 3.5 Hz, 2H), 7.47 (s, 1H), 7.46 (s, 1H), 7.36–7.28 (m, 5H), 5.79 (s, 2H), 1.83 (s, 9H), 1.78 (s, 9H), 1.71 (s, 9H) ppm. ^{13}C-NMR (126 MHz, $CDCl_3$): δ = 153.2 (C_q), 151.3 (C_q), 151.0 (C_q), 150.5 (C_q), 149.2 (C_q), 148.8 (C_q), 138.0 (C_q), 137.6 (C_q), 137.3 (C_q), 135.0 (C_q), 134.3 (C_q), 134.1 (C_q), 129.0 (CH), 127.7 (CH), 126.9 (CH), 126.4 (CH), 126.3 (CH), 122.2 (CH), 122.2 (CH), 121.4 (C_q), 121.1 (C_q), 117.7 (C_q), 117.4 (C_q), 116.8 (C_q), 115.0 (C_q), 113.3 (C_q), 113.2 (C_q), 112.7 (C_q), 112.7 (C_q), 106.8 (CH), 105.1 (2 × CH), 47.8 (CH_2), 35.6 (C_q), 35.5 (C_q), 35.4 (C_q), 30.7 (CH_3), 30.6 (CH_3), 30.4 (CH_3) ppm. MALDI HRMS: calcd for $C_{47}H_{41}NO_3$ $[M]^+$ *m*/*z* 667.30864, found 667.30724.

***N*-Benzyl-tri-*tert*-butyl-methoxy-azatrioxa[8]circulene, 2$_{tBuOMe}$.** *N*-Benzyl-2,7-di-*tert*-butyl-9*H*-carbazole-3,6-diol (200 mg: 0.50 mmol) and 2-tertbutyl-1,4-benzoquinone (82 mg: 0.50 mmol) was dissolved in CH_2Cl_2 (50 ml) and placed under a nitrogen atmosphere. BF_3OEt_2 (0.13 ml: 1.00 mmol) was added to the reaction mixture and the reaction mixture was stirred for 5 hours. 2-Methoxy-1,4-benzoquinone (103 mg: 0.75 mmol) was added and the reaction mixture was stirred overnight. The reaction was quenched using 1 M HCl (100 ml) followed by the addition of KOH pellets until the water phase was alkaline. Extraction with CH_2Cl_2 (4 × 50 ml) was performed and the combined organic phase was dried over anhydrous Na_2SO_4 and filtered. The solvent was removed under vacuum and the brown crude product was purified by dry column vacuum filtration [id 4 cm; 4 cm silica; 50 cm^3 fractions, 0–22% toluene in heptane(v/v), 2% increments] yielding *N*-benzyl-tri-*tert*-butyl-methoxy-azatrioxa[8]circulene (**10**), as a fine yellow powder.

Yield: 43% (139 mg: 0.21 mmol) melting point: 326–329 °C TLC: R_f -value = 0.66 (toluene/*n*-heptane, 1 : 4) ^{1}H-NMR (500 MHz, $CDCl_3$): δ = 7.75 (s, 1H), 7.39 (s, 1H), 7.36 (s, 1H), 7.34 (s, 1H), 7.33–7.27 (m, 5H), 5.74 (s, 2H), 4.25 (s, 3H, O-CH_3), 1.76 (s, 9H), 1.68 (s, 9H) ppm. ^{13}C-NMR (126 MHz, $CDCl_3$): δ = 153.3 (C_q), 153.0 (C_q), 151.8 (C_q), 151.1 (C_q), 150.8 (C_q), 145.8 (C_q), 142.7 (C_q), 138.0 (C_q), 137.5 (C_q), 137.3 (C_q), 135.3 (C_q), 134.2 (C_q), 134.2 (C_q), 129.0 (*C*H), 127.6 (*C*H), 126.8 (*C*H), 117.6 (C_q), 117.2 (C_q), 117.0 (C_q), 116.6 (C_q), 115.3 (C_q), 112.7 (C_q), 112.3 (C_q), 110.0 (C_q), 107.8 (*C*H), 105.5 (*C*H), 104.4 (*C*H), 94.9 (*C*H), 57.2 (O–*C*H_3), 47.7 (*C*H_2), 35.5 (C_q), 35.4 (2 × C_q), 30.5 (*C*H_3), 30.5 (*C*H_3), 30.4 (*C*H_3) ppm. MALDI HRMS: calcd for $C_{44}H_{41}NO_4$ $[M]^+$ *m*/*z* 647.30356, found 647.30208.

***N*-Benzyl-tri-*tert*-butyl-dodecylthio-azatrioxa[8]circulene, 2$_{tBuSDo}$.** *N*-Benzyl-2,7-di-*tert*-butyl-9*H*-carbazole-3,6-diol (100.4 mg: 0.25 mmol) was dissolved in CH_2Cl_2 (15 ml) followed by the addition of a solution of 2-*tert*-butyl-1,4-quinone (41.6 mg: 0.25 mmol) in CH_2Cl_2 (5 ml) and BF_3OEt_2 (0.06 ml: 0.50 mmol). The reaction was placed under a nitrogen atmosphere and stirred using magnetic stirring. After 5 hours 2-dodecylthio-1,4-quinone (115.6 mg: 0.38 mmol) dissolved in CH_2Cl_2 (5 ml) was added. The reaction mixture was again placed under a nitrogen atmosphere and stirred using magnetic stirring. After 68 hours of additional stirring, the reaction was quenched using 1 M HCl (50 ml). KOH-pellets were added until the water phase was alkaline. Extraction with CH_2Cl_2 (4 × 50 ml) was performed and the combined extracts were dried using Na_2SO_4 and filtered. The solvent was removed under vacuum and the yellow-brown crude product was purified by

dry column vacuum chromatography [id 4 cm; 3 cm silica; 100 cm3 fractions; 5–13% toluene in heptane (v/v) – 2% increments] yielding *N*-benzyl-tri-*tert*-butyl-dodecylthio-azatrioxa[8]circulene (**11**) as a yellow solid.

Acknowledgements

We acknowledge financial support from the Lundbeck Foundation for a Young Group Leader Fellowship (MP), the Villum foundation for a diffractometer for determining the single crystal X-ray structures and the Danish high technology foundation. We thank Dr Sophie R. Beeren for insightful discussions.

Notes and references

1 R. Breslow, *Acc. Chem. Res.*, 1973, **6**, 393–398.
2 *Carbon-Rich Compounds*, ed. M. M. Haley and R. R. Tykwinski, Wiley-VCH, Weinheim, 2006.
3 (*a*) *Functional Organic Materials*, ed. T. J. J. Muller and U. H. F. Bunz, Wiley-VCH, Weinheim, 2007; (*b*) *Organic Light Emitting Devices: Synthesis Properties and Applications*, ed. K. Müllen and U. Scherf, Wiley-VCH, Weinheim, 2006.
4 D. T. Chase, A. G. Fix, B. D. Rose, C. D. Weber, S. Nobusue, C. E. Stockwell, L. N. Zakharov, M. C. Lonergan and M. M. Haley, *Angew. Chem., Int. Ed.*, 2011, **50**, 11103–11106.
5 S. Mori and A. Osuka, *J. Am. Chem. Soc.*, 2005, **127**, 8030–8031.
6 M. Ishida, S.-J. Kin, C. Preihs, K. Ohkubo, J. M. Lim, B. S. Lee, J. S. Park, V. M. Lynch, V. V. Roznyatovskiy, T. Sarba, P. K. Panda, C.-H. Lee, S. Fukuzumi, D. Kim and J. L. Sessler, *Nat. Chem.*, 2012, **5**, 15–20.
7 M. Stephien, L. Latos-Grażyński and L. Szterenberg, *J. Org. Chem.*, 2007, **72**, 2259–2270.
8 A. Matsuura and K. Komatasu, *J. Am. Chem. Soc.*, 2001, **123**, 1768–1769.
9 S. Miao, S. M. Brombosz, P. v. R. Schleyer, L. I. Wu, S. Barlow, S. R. Marden, K. I. Hardcastle and U. H. F. Bunz, *J. Am. Chem. Soc.*, 2008, **130**, 7339–7344.
10 Y. Nakamura, N. Aratani, H. Shinokubo, A. Takagi, T. Kawai, T. Matsumoto, Z. S. Yoon, D. Y. Kim, T. K. Ahn, D. Kim, A. Muranaka, N. Kobayashi and A. Osuka, *J. Am. Chem. Soc.*, 2006, **128**, 4119–4127.
11 K. Y. Chernichenko, V. V. Sumerin, R. V. Shpanchenko, E. S. Balenkova and V. G. Nenajdenko, *Angew. Chem., Int. Ed.*, 2006, **45**, 7367–7370.
12 X. Xiong, C.-L. Deng, B. F. Minaev, G. V. Baryshnikov, X.-S. Peng and H. N. C. Wong, *Chem. – Asian J.*, 2014, **10**, 969–975.
13 J. Eskildsen, T. Reenberg and J. B. Christensen, *Eur. J. Org. Chem.*, 2000, 1637–1640.
14 (*a*) H. G. H. Erdtman, *Proc. R. Soc. London., Ser A*, 1933, **143**, 228–241; (*b*) H. G. H. Erdtman and H.-E. Högberg, *Chem. Commun.*, 1968, 773–774; (*c*) H. Erdtman and H.-E. Högberg, *Tetrahedron Lett.*, 1970, **11**, 3389–3392; (*d*) H.-E. Högberg, *Acta Chem. Scand.*, 1973, **27**, 2559–2566.
15 (*a*) T. Hensel, D. Trpcevski, C. Lind, R. Grosjean, P. Hammershøj, C. B. Nielsen, T. Brock-Nannestad, B. E. Nielsen, M. Schau-Magnussen, B. F. Minaev, G. V. Baryshnikov and M. Pittelkow, *Chem. – Eur. J.*, 2013, **19**, 17097–17102; (*b*) C. B. Nielsen, T. Brock-Nannestad, P. Hammershøj, T. K. Reenberg, M. Schau-Magnussen, D. Trpcevski, T. Hensel, R. Salcedo, G. V. Baryshnikov, B. F. Minaev and M. Pittelkow, *Chem. – Eur. J.*, 2013, **19**, 3898–3904.
16 (*a*) G. V. Baryshnikov, R. R. Valiev, N. N. Karaush and B. F. Minaev, *Phys. Chem. Chem. Phys.*, 2014, **16**, 15367–15374; (*b*) G. V. Baryshnikov, B. F. Minaev, M. Pittelkow, C. B. Nielsen and R. Salcedo, *J. Mol. Model.*, 2013, **19**, 847–850.
17 C. B. Nielsen, T. Brock-Nannestad, T. K. Reenberg, P. Hammershøj, J. B. Christensen, J. W. Stouwdam and M. Pittelkow, *Chem. – Eur. J.*, 2010, **16**, 13030–13034.
18 T. Brock-Nannestad, C. B. Nielsen, M. Schau-Magnussen, P. Hammershøj, T. K. Reenberg, A. B. Petersen, D. Trpcevski and M. Pittelkow, *Eur. J. Org. Chem.*, 2011, 6320–6325.
19 H.-E. Högberg, *Acta Chem. Scand.*, 1972, **26**, 2752–2758.
20 M. A. Christensen, C. R. Parker, T. J. Sørensen, S. de Graaf, T. J. Morsing, T. Brock-Nannestad, J. Bendix, M. M. Haley, P. Rapta, A. Danilov, S. Kubatkin, O. Hammerich and M. B. Nielsen, *J. Mater. Chem. C*, 2014, **2**, 10428–10438.